Pharm Res (2011) 28:494–504
DOI 10.1007/s11095-010-0247-y

RESEARCH PAPER

Investigating the Effect of Polymeric Approaches on Circulation Time and Physical Properties of Nanobubbles

Lisa C. du Toit • Thirumala Govender • Viness Pillay • Yahya E. Choonara • Tetsuya Kodama

Received: 19 March 2010 / Accepted: 13 August 2010 / Published online: 23 December 2010

ABSTRACT

Purpose A challenge in the field of nanobubbles, including lipobubbles and polymeric nanobubbles, is identification of formulation approaches to enhance circulation time or "bubble life" in the specific organ to allow for organ visualization. The aim of this study was to investigate the potential of two specific preparation approaches, polymeric surface modification to lipobubbles and a one-step approach for the preparation of ionotropically originated polymeric hydrogel nanobubbles for the production of biocompatible, biodegradable, and sufficiently echogenic ('flexible') bubbles, preferably within the nanometer range, that possess an enhanced *in vivo* lifetime compared to an unmodified lipobubble to allow visualization of the lymph node vasculature.

Methods In the first approach, formed liposomes (basic and polymerically enhanced) were sequentially layered with appropriate cationic and anionic polyelectrolytes followed by transformation into polymer-coated nanobubbles. In addition, a one-step approach was employed for the fabrication of ionotropically originated polymeric hydrogel bubbles.

Results Bubble lifetime was marginally enhanced by self-deposition of polyelectrolytes onto the normal lipobubble, however, not significantly ($P = 0.0634$). In general, formulations possessing a higher ratio of anionic:cationic coats and highly anionic overall surface charge (−20.62 mV to −17.54 mV) possessed an enhanced lifetime. The improvement in bubble lifetime was significant when a purely polymeric polyionic hydrogel bubble shell was instituted compared to a normal unmodified lipobubble ($P = 0.004$). There was enhanced persistence of these systems compared to lipobubbles, attributed to the highly flexible, interconnected hydrogel shell which minimized gas leakage. The prolonged contrast signal may also be attributed to a degree of polymeric deposition/endothelial attachment.

Conclusions This study identified the relevance of polymeric modifications to nanobubbles for an improved circulating lifetime, which would be essential for application of these systems in passive drug or gene targeting via the enhanced permeability and retention effect.

KEY WORDS hydrogel · layer-by-layer self-deposition · liposome · nanobubble · polymer

L. C. du Toit · V. Pillay · Y. E. Choonara
Department of Pharmacy and Pharmacology
University of the Witwatersrand
7 York Road, Parktown
2193 Johannesburg, South Africa

T. Govender
School of Pharmacy and Pharmacology, University of KwaZulu Natal
Durban, South Africa

T. Kodama (✉)
Graduate School of Biomedical Engineering, Tohoku University
2-1 Seiryo-machi, Aoba
Sendai 980-7583, Japan
e-mail: kodama@bme.tohoku.ac.jp

INTRODUCTION

Nanobubbles are recent nanostructures and are termed as such since their internal core surrounded by a shell/membrane is gas-filled. The shell membrane of nanobubbles consists of albumin, lipid or biocompatible polymer for the purpose of stability enhancement against gas loss, dissolution, bubble coalescence and the attainment of an improved particle size distribution (1). The internal gas core comprises either air or perfluorocarbons. The presence of a gas core, specifically, confers the capability of *in vivo*

tracking of the system via ultrasound imaging. These 'acoustic' spheres are being increasingly investigated in the literature for simultaneously achieving targeted drug/gene delivery and organ imaging (1,2). This nanocarrier delivery system therefore has potential applications in diverse diseases, such as cancer, atherosclerosis, Alzheimers disease, HIV/AIDS and genetic diseases, such as diabetes.

Specifically, liposomal and polymeric nanobubble systems are being extensively explored due to their potential to serve as biocompatible delivery vehicles for both hydrophobic and hydrophilic drugs, to be retained within tissues of interest and for allowing their visualization for disease monitoring as ultrasound contrast agents (3). Contrast-enhanced ultrasound describes the application of ultrasound contrast medium to traditional medical sonography, which is an ultrasound-based diagnostic imaging technique employed to visualize subcutaneous body structures. Nanobubbles are useful as contrast agents for ultrasound imaging because the magnitude of their acoustic backscatter can be significantly greater than the backscatter of blood and the majority of other tissues and organs. This is due to the high acoustic impedance mismatch between gases and blood or soft tissue (1). A current challenge in the field of nanobubbles is identification of formulation approaches that can enhance their circulation time or 'bubble life' in the specific organ to allow adequate time for organ visualization. For example, liposomal bubbles possess a high tendency to degrade or aggregate and fuse with the resultant leakage of the entrapped drug during storage or after administration, rendering their *in vivo* stability a topic of concern (3). Hernot and Klibanov (1) recently emphasized that stiffness of the bubbles, their resistance to rupture in the ultrasound pressure field, and the ease with which they are recognized and cleared by the reticuloendothelial system rest on the composition of the bubble shell.

To address these challenges, a number of approaches have been investigated, such as liposomal size variation or liposomal surface modification via coating with a single layer of hydrophilic polymers (4–6). Emerging innovative approaches include the concept of polyelectrolyte coatings obtained by the alternate deposition of polyanions and polycations for surface functionalization (7). Multilayer films of organic compounds by consecutive adsorption of polyanions and polycations on solid surfaces allow fabrication of multicomposite molecular assemblies of tailored architecture (8).

While Haidar *et al.* (7) recently reported a layer-by-layer (LbL) technique of alternate deposition of polymers on liposomes for enhancing stability, this approach has not been widely employed for lipobubbles or for any other nanobubble system to date. It should be further noted that in employing the above layering approach, contravening results have been reported, since polymer-coated liposomes showed little or less stability than non-coated liposomes (3). To clarify the effectiveness of polymer coatings on the physical stability of liposomes, further information is required, especially with respect to the relationship between properties of coatings and improvement in stability of liposomes (3). This may be determined via *in vivo* imaging techniques.

In addition to lipobubbles, various purely polymeric bubble systems are being reported in alternative attempts to attain improved stability and prolonged *in vivo* persistence, (9–14). Air-filled particles with a polymeric shell are purported to exhibit a longer persistence after injection than a nonpolymeric microbubble and may be suitable for organ and peripheral vein imaging (14). A variety of natural and synthetic polymers have been employed to encapsulate imaging contrast agents (14); however, the shortcomings to date are apparent. These include poor encapsulation of gaseous imaging contrast agents, poor *in vivo* stability, large size limiting capillary passage and precluding targeting via the EPR effect (15), low echogenicity and the use of organic solvents (9–14).

There thus remains a need to identify and optimize different methods for production of biocompatible, biodegradable and sufficiently echogenic ('flexible') nanobubbles with a reproducible size range and with enhanced *in vivo* stability (bubble life time). This would be essential to realise the applicability in contrast imaging and/or drug delivery. This investigation also considered the synthesis of crosslinked polyionic hydrogel micro-/nanobubbles, inherent in which are the principles of ionotropic gelation/complexation between at least two polyionic species for the formation of an interconnected polyionic hydrogel for gas encapsulation. The distinctive combination of chitosan and sodium alginate has been highlighted as the most applicable for colloidal carrier systems (16–18). The implementation of this system for the creation of micro-/nanobubbles for contrast-enhanced ultrasound has, to our knowledge, not yet been significantly reported in the literature. In addition to the use of chitosan and alginate as polymers, the potential of the anionic thermoresponsive polymer, poly(*N*-isopropylacrylamide) (PNIPAM), which is well-known to exhibit a thermo-responsive phase transition at 32−33°C in aqueous solution, was also explored (19). Thus, in addition to selective accumulation of the nanobubble system at a solid tumor by a passive targeting mechanism, a thermo-responsive system is also able to increase the spatial specificity in combination with a physical targeting mechanism. This may be achieved by the introduction of a thermo-responsive polymer segment, such as PNIPAM (20). Also under investigation in this study, as a potential anionic polymer, is the extensively studied tissue adhesive poly(alkyl cyanoacrylate) (PACA), which has been employed as a polymeric colloidal drug carrier obtained via simple polymerization reactions.

The aim of this study was therefore to investigate the potential of two specific preparation approaches, i.e. polymeric surface modification to lipobubbles and an alternative innovative one-step approach for the preparation of ionotropically originated polymeric hydrogel nanobubbles for the production of bubbles, preferably within the nanometer range and possessing an enhanced *in vivo* lifetime compared to an unmodified lipobubble to allow visualization of the lymph node vasculature. The size, surface charge and *in vivo* lifetime of the bubbles (determined via ultrasound imaging of their retention in perivascular lymph tissue following injection into MRL/lpr mice (21)), which develop systemic lymphadenopathy generated via the described approaches, were compared to an unmodified/basic lipobubble to identify a suitable bubble system that would demonstrate enhanced persistence for enabling visualization of the mouse lymph node vasculature over a sufficient period of time.

MATERIALS AND METHODS

Materials

Distearoylphosphatidyl choline (DSPC; Coatsome MC 8080) and distearoylphosphatidyl-ethanolamine-poly(ethylene glycol) (DSPE-020C) were purchased from NOF Corporation (Japan). Dulbecco's phosphate- buffered saline (DPBS) was purchased from Sigma-Aldrich® (St. Louis, USA). Chloroform and methanol were purchased from Wako Pure Chemical Industries, Ltd. (Japan). Chitosan (low molecular weight, $M_w < 6000$ Da, viscosity ~20 000 cps), alginic acid (sodium salt) (20,000−40,000 cps), and poly(*N*-isopropyl-acrylamide) ($M_w = 20{,}000–25{,}000$ Da) were purchased from Sigma-Aldrich® (Sigma-Aldrich®, St. Louis, USA). Butyl-2-cyanoacrylate (Histoacryl®) was purchased from Braun, Aesculup, Tuttlingen).

Preparation of Polymer-Coated Lipobubbles

The first approach investigated combined the advantageous properties of liposomes transformed into nanobubbles for contrast-enhanced ultrasound, with the stability-enhancing potential of hydrophilic biodegradable biocompatible polymers. The formed liposomes (basic and polymerically enhanced) were sequentially layered with appropriate cationic and anionic polyelectrolytes. The multilayered liposomes were then transformed to polymer-coated nanobubbles.

Preparation of the Basic Liposomal Suspension

Liposomes were prepared in accordance with a reverse phase methodology. In this approach, two phospholipids (DSPC and DSPE) were dissolved in an organic solvent phase of chloroform:methanol (9 mL:1 mL) in a pear-shaped flask (the phospholipids were stored at −20°C and placed on a dessicator 30–60 min prior to liposome preparation). This was followed by addition of the aqueous phase (DPBS). Sonication (to achieve liposome sizing) of the two-phase system was undertaken with a probe sonicator (VibraCell, Sonics and Materials, Inc., Danbury, CT, USA) until the mixture became a one-phase dispersion. The mixture was then placed on the rotary evaporator (Eyela, Tokyo, Japan) with the water bath temperature maintained at 65°C (boiling point of chloroform ~62°C) and the lower pressure limit kept within the range of 200-100 hPa. The mixture was occasionally vortexed with the addition of 500 μL of PBS until all the organic solvent was removed and the liposomal suspension was formed. The volume of the solution was adjusted to about 5 mL with PBS (22).

Following formation of the crude liposomal suspension, it was subjected to 3−5 freeze-thaw cycles (freezing with 150 mL acetone: dry ice and thawing at 37°C). This was necessary for conversion of the multilamellar vesicles, formed upon phase exchange, to unilamellar vesicles. Uniform sizing of the liposomes was achieved with an extruder device (Eyela, Tokyo, Japan), employing a membrane pore size of 600 nm × 2 times, 200 nm × 5 times, and 100 nm × 10 times. The device was maintained at 60°C. Conversion of the basic liposomes to basic lipobubbles (which served as the control) was as per the approach described in "Conversion of Basic and Polymer-Coated Liposomes to Basic and Polymer-Coated Lipobubbles."

Preparation of Polymerically-Enhanced Liposomes

Formation of the polymerically enhanced liposome involved preparation of a lipid film via solvent evaporation. It employed formulatory components as described for the reverse phase methodology for liposome preparation. DSPC and DSPE were dissolved in chloroform:methanol (9 mL:1 mL) in a pear-shaped flask followed by evaporation of the organic solvent with a rotary evaporator to form a lipid film on the inside of the flask. Five mL of a 1 mg/mL alginic acid or PNIPAM solution were then added to the lipid film with subsequent vortexing to generate a polymeric liposomal mixture. Sizing of the mixture was then undertaken via extrusion as described in "Preparation of the Basic Liposomal Suspension."

Preparation of Polymer-Coated Lipobubbles

Preparation of Polymer Solutions. Liposomes were sequentially layered with polymeric solutions of the cationic polymer, chitosan, anionic polymers, naturally derived alginic acid and synthetic thermoreversible poly(N-isopropyl-acrylamide) (PNIPAM). The polymer solutions were

prepared as follows: Twenty mg of low molecular weight chitosan was dissolved in 6 mL deionised water and 0.1 mL 1 N HCl overnight. Six mL DPBS was added to the solution (pH ~5.5). The pH of the solution was adjusted to 6.6 with the addition of 1 N NaOH. The final solution was vortexed. The anionic alginate solution was prepared by dissolution of 25 mg alginic acid (sodium salt) in 50 mL DPBS. Preparation of the PNIPAM solution entailed dissolution of 10 mg of the polymer in 10 mL DPBS at 25°C.

Sequential Polymeric Layer-by-Layering (LbL) of Liposomes. To achieve the LbL coating of normal and polymerically enhanced liposomes, 1 ml of the polymer solution (layer 1 in Table 1) was added to 1 mL of the prepared liposome solution (possessing a phospholipid concentration of 18.61 mg/mL). The mixture was left overnight at room temperature (25°C) for 12 h to affect self-deposition of the polymer onto the negatively charged liposomal surface, at which point particle size analysis was undertaken, employing a Zeta potential and particle size analyser (ELSZ-2, Otsuka Electronics, Osaka, Japan). Thereafter, 0.4 mL of the second polymer solution (layer 2 in Table 1) was added to the polymer-coated nanoliposomal mixture and left to deposit on the previous layer over 4 h, at which time the size was measured. Consecutive layers were incorporated via the addition of 0.2 mL of the respective polymeric solutions. After 4 h to allow for polymeric deposition, the size of the liposomes was measured. Following deposition of the final layer, the polymer-coated liposomes were converted to lipobubbles as per the approach described in "Conversion of Basic and Polymer-Coated Liposomes to Basic and Polymer-Coated Lipobubbles," and the final size was measured. The various combinations of polymer layers for both the basic and polymerically enhanced lipobubbles are shown in Table 1.

Conversion of Basic and Polymer-Coated Liposomes to Basic and Polymer-Coated Lipobubbles. The following was undertaken to affect coversion of the basic liposomes and polymer-coated liposomes to basic lipobubbles and polymer-coated lipobubbles. One mL of the liposomal formulations was exposed, with sonication in 7 mL vials, to perfluorocarbon (C_3F_8) gas for 1 min. This resulted in replacement of the aqueous core with a gaseous core. All polymer surface-modified lipobubble formulations were prepared at least in triplicate ($n=3$) for evaluation.

Preparation of Polymeric Bubbles

An innovative one-step approach was employed for the preparation of ionotropically originated polymeric hydrogel micro-/nanobubbles. It is thus proposed that a polyionic nanogel following mixing of appropriately selected biodegradable, biocompatible polymers in the presence of a gas of sufficient echogenicity would lead to the formation of a crosslinked polyionic micro-/nanobubble possessing sufficient stability and *in vivo* persistence, echogenicity and suitable size distribution. This approach to formation of nanobubbles would widen the pool of available methods and polymeric systems for preparation of polymeric nanobubbles and would also enable identification of their suitability for targeting and imaging.

This approach explored the formation of two types of polymeric nanobubbles. The first entailed the interaction of synthesized PBCA nanobubbles with chitosan to form a composite polyionic bubble structure. The second method involved interaction of dilute solutions of oppositely charged polymeric species to form polyionic hydrogel nanobubbles.

Preparation of Air-Filled Poly(butyl-2-cyanoacrylate) Nanobubbles. Initially, poly(cyano acrylate) nanobubbles were prepared as a component of the polyionic hydrogel bubbles. The synthesis of air-filled surfactant-stabilised poly(cyano acrylate) nanobubbles was undertaken in accordance with a method adapted from Schmidt and Roessling (23) and Palmowski *et al.* (24). One-half mL monomeric butyl-2-cyanoacrylate (Histoacryl®, Braun, Aesculup, Tuttlingen) was added to an aqueous 0.01 M HCl solution (pH 2.25) containing 0.02%v/v Tween®20. This was followed by vigorous agitation for 1 h that resulted in a nanobubble suspension. Neutralisation of the nanobubble suspension was undertaken via the addition of an equal volume of DPBS (pH 7.4). Sodium hydroxide (1 M) was then added to achieve a pH of 7.0 to obtain the final poly(butyl-2-cyanoacrylate) (PBCA) nanobubble suspension. The PBCA nanobubble size attained was 124.7 ± 31.0 nm. The suspension was filtered under sterile conditions.

Preparation of Polyionic Hydrogel Bubbles. The concentrations of the respective polymers employed were preliminarily identified such that an opalescent suspension would be formed when the opposing polymers were mixed (in contrast to a clear solution or aggregates) (Figures 1 and 2).

The PBCA nanobubble suspension was prepared as described above. 0.3% w/v alginic acid, or 0.3% alginic acid and 0.15% PNIPAM solutions incorporating 0.02% v/v Tween® 20 were prepared in DBPS (pH 7.4). A 0.15% w/v chitosan solution, 0.04% v/v Tween® 20 solution was prepared. All solutions prepared were subjected to sterile filtration. Following brief sonication (10 s) of 1 mL aqueous solution of the polycation (20 kHz sonicator, VibraCell, Sonics and Materials, Inc., Danbury, CT, USA), 1 mL of

Table I Polymer-Coated Lipobubble Formulations

Formulation	Basic liposome	Polymeric-enhancement liposome	Layer 1	Layer 2	Layer 3	Layer 4
Control	Yes	–	–	–	–	–
A1	Yes	–	Chitosan	Alginate	Chitosan	Alginate
A2	Yes	–	Chitosan	PNIPAM	Chitosan	PNIPAM
A3	Yes	–	Alginate	Chitosan	Alginate	–
A4	Yes	–	PNIPAM	Chitosan	PNIPAM	
A5	–	Yes	–	–	–	–
A6	–	Yes	PNIPAM	–	–	–
A7	–	Yes	Chitosan	PNIPAM	–	–

the polyanionic solution or suspension was sprayed into the polycation in the presence of perfluorocarbon gas with further sonication for 1 min (Figure 3). The interaction between the carboxyl or hydroxyl groups of the anionic polymer and the amine groups of chitosan formed an immediate polyionic micro-/nanogel, which entrapped the gas. Three formulations (Table 2) were designed for evaluation. In the case of the chitosan-PBCA, deposition of hydrophobic PBCA nanobubbles at the superficial chitosan microbubble layers formed a gas-tight film. All formulations were prepared at least in triplicate ($n=3$) for evaluation.

Nanobubble Size and Stability Analysis

The size distribution, average diameter and zeta potential of the nanobubbles were assessed, employing an electron light scattering device (ELSZ-2) before injection. All measurements were performed in triplicate ($n=3$).

In Vivo Assessment of Nanobubble Lifetime: Microultrasound Imaging

A high-frequency microultrasound imaging system (Vevo 770®, VisualSonics, Toronto, Canada) designed specifical-

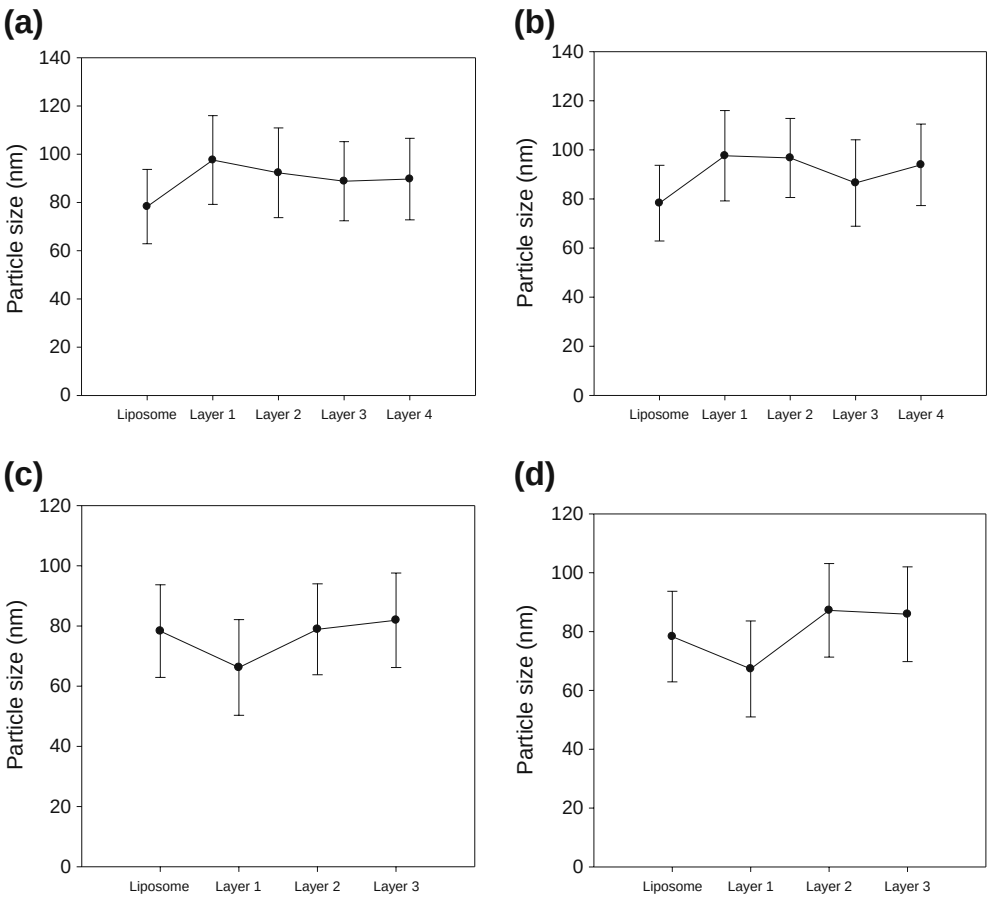

Figure 1 Effect on liposome size following LbL self-deposition of polyelectrolytes onto the normal liposome for formulations (**a**) A1 showing a decrease in particle size from layer 1 to 2 due to complexation between consecutive oppositely charged polymeric layers (chitosan and alginate), (**b**) A2 demonstrating a decrease in particle size from layer 2 to 3 due to enhanced polymeric interpenetration between PNIPAM and chitosan at this stage, (**c**) A3 showing a dramatic decrease in size on application of the first layer to the liposome attributed to the anionic polymeric chains adsorbing tightly around the phospholipid bilayer instigating shrinkage of the liposomal structure and (**d**) A4 also demonstrating a sharp decrease in particle size on initial polymeric layering with a subsequent dramatic increase in size with layer 2.

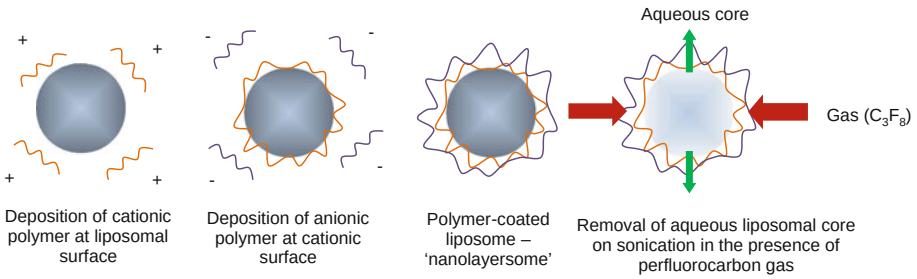

Figure 2 Creation of a polymer-coated liposome by layer-by-layer self-deposition and polymer-coated lipobubble formation.

ly for imaging small animals was used in these studies. Contrast mode images were acquired at a broadband frequency of 60 MHz (scanhead RMV 704) (with axial and lateral resolutions of 40 µm and 80 µm, respectively). Cine loops of approximately 300 frames were collected for each experiment at a frame rate of 15 Hz.

MRL/lpr mice were employed for *in vivo* detection of the total bubble lifetime in the lymph node vasculature. Ethics clearance was obtained from the relevant committee at Tohoku University. Mice were anaesthetised in a chamber with 2% isoflurane gas in oxygen. Body temperature was maintained at 37°C using a heat pad. Mice were placed supine on the imaging stage. Their fore- and hindlegs were extended, placed on electrode gel and taped to the stage to monitor respiration (and minimize respiration motion). Lymph nodes were imaged at the widest cross-section, and the transducer was fixed with a three-dimensional (3-D) stage control system (Mark-204-MS; Sigma Koki, Tokyo, Japan). Two-hundred µL of the bubble suspension was caudally injected and visualized within the lymph node via a bioimaging system (Vevo® 770, VisualSonics, Toronto, Canada). The time (in minutes) during which the vascular architecture could be clearly visualized as a result of the acoustic signal generated by the bubbles was compared for the formulations, and reported as the 'bubble lifetime.' Bubble lifetime measurements were conducted in duplicate ($n=2$).

Statistical Analysis

The significance of the improvement in the nanobubble lifetime of the various synthesized forms compared to basic lipobubbles (control) was assessed via one-way ANOVA tests (SigmaPlot, V11, Systat Software Inc., San Jose/Chicago, USA). A P value of <0.05 was considered significant. Linear regression analyses were undertaken using Windows XP Microsoft Excel Macros (Add-Ins).

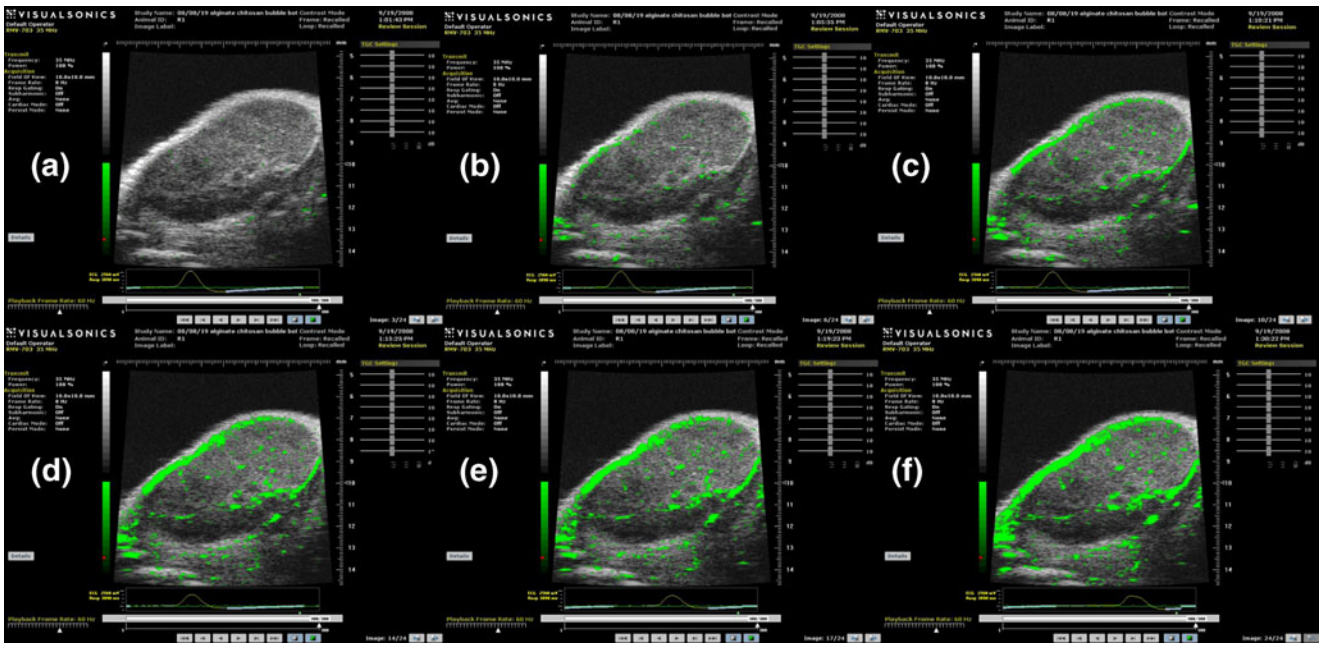

Figure 3 Vascular contrast enhancement following injection of formulation B1 into the subiliac lymph node of the MRL/lpr mouse at (**a**) 1 min, (**b**) 5 min, (**c**) 10 min, (**d**) 15 min, (**e**) 20 min, (**f**) 30 min. The progressively enhanced contrast is noted.

Table 2 Composition of the Polyionic Hydrogel Bubbles

Formulation	Polycationic composition	Polyanionic composition		
	Chitosan (%w/v)	Alginic acid (%w/v)	PBCA (%v/v)	PNIPAM (%w/v)
B1	0.15	0.3	–	–
B2	0.15	–	2.5	–
B3	0.15	0.3	–	0.15

RESULTS

Nanobubble Size and Stability Analysis

Polymer-Coated Lipobubble Characterization

The particle size of the basic lipobubble (control), i.e. non-surface-modified, was 78.3 nm. The normal size range of basic lipobubbles obtained in previous investigations employing this methodology is <100 nm (2). LbL coating onto the basic liposomes (A1-A4) caused a gradual increase in the liposomal diameter (Figures 1 and 2, Table 3), although strong complexation between oppositely charged polymeric layers or the liposomal surface and polymeric chains may be responsible for the decrease in diameter observed with certain layers (Figure 1). The size remained within the nanometer range upon conversion to the lipobubble, which followed application of the final layer (81.9 nm to 93.9 nm, PdI = 0.217–0.546). The zeta potential of formulations via the process of self-deposition ranged from −20.62 mV to 0.54 mV.

Polyionic Hydrogel Bubble Characterization

Depending on the formulatory approach, the inherent characteristics of the polyionic hydrogel bubbles varied considerably in terms of their size and surface charge properties (Table 3). Being nanogels, these systems displayed a tendency to increase in size on standing (except for the chitosan-PBCA system). The size of the bubbles was thus assessed immediately after preparation and before injection into the mouse (i.e. 60 min after preparation). The initial sizes of the bubbles were 508.9 ± 58.4 nm, 641.7 ± 65.7 nm, and 993.9 ± 973.8 nm, for B1, B2, and B3, respectively. Thereafter, there was a substantial transition in size as the bubbles generally stood for up to 60 min prior to injection (Table 3).

Bubble Lifetime with Reference to Basic Lipobubbles

Polymer-Coated Lipobubble Characterization

The bubble lifetime of the control lipobubble was 5 min. Bubble lifetime was somewhat enhanced by LbL self-deposition of polyelectrolytes onto the normal lipobubble (Table 3) as the bubble lifetimes ranged from 5 to 9 min.

Polyionic Hydrogel Bubble Characterization

Bubble lifetimes of 30, 40 and 25 min were attained for formulations B1, B2, and B3, respectively (Table 3, Figures 3 and 4). The proposed transitory configuration of polyionic hydrogel bubbles, which may have contributed to the observed prolongation of bubble lifetime, is depicted in Figure 5.

DISCUSSION

Nanobubble Size and Stability Analysis

Polymer-Coated Lipobubble Characterization

Particle size and zeta potential are important parameters for the characterization of a nanosystem. It has long been known that pure bubbles have a negatively charged surface in pure water. First, the resultant bubble size has important implications on system applicability. Formulations possessing a size range of ~200 nm will have applicability for imaging and drug and gene delivery via the EPR effect. The zeta potential of a particle is the overall charge that the particle acquires in a particular medium. The magnitude of the measured zeta potential is an indication of the repulsive force that is present and ultimately the long-term stability of the product. The presence of a large negative or positive zeta potential highlights the propensity of the particles in suspension to repel each other with little tendency for aggregation or flocculation.

It is noteworthy that the adsorption of the second anionic layer, i.e. layer 3, on a previously adsorbed chitosan layer, where chitosan forms layer 1, caused a decrease in the mean particle size, which is especially noticeable with the first two layers, stabilizing thereafter (noted for formulations A1 and A2) (Figure 1). This behavior might be explained by the ability of the shorter polymer chains of the negatively charged polyelectrolytes to easily diffuse between the longer polymer chains of chitosan due to the strong ionic electrostatic interactions and complexation of the polymers forming a denser network.

Table 3 Characteristics of Polymer-Coated Lipobubbles and Polymeric Hydrogel Bubbles

Formulation	Bubble diameter before injection (nm)	Zeta potential (mV)	Bubble lifetime (minutes)	Improvement in bubble lifetime compared to basic lipobubble (%)
Control	78.3 ± 2.11	−20.48 ± 1.64	5	–
A1	89.7 ± 6.28	0.54 ± 0.016	5	0
A2	93.9 ± 5.16	−2.83 ± 0.20	5	0
A3	81.9 ± 6.72	−12.56 ± 0.83	7	40
A4	85.9 ± 2.58	−15.40 ± 0.83	9	80
A5	82.5 ± 7.76	−20.62 ± 0.41	8	60
A6	87.4 ± 3.50	−18.23 ± 2.01	5	0
A7	91.1 ± 2.46	−5.77 ± 0.21	5	0
B1	4124.0 ± 295.4	−28.89 ± 6.63	30	500
B2	255.0 ± 62.7	−27.23 ± 5.93	40	700
B3	6743.6 ± 1231.9	−34.55 ± 6.72	25	400

The anionic fractions (DSPE, alginic acid and PNIPAM have a negative surface charge which is pH-dependent) contributed to the resultant negativity to the surface charge. DSPC exhibits no net charge, whereas chitosan makes a significant contribution to the positivity of the surface. Overall formulations possessed a net negative charge as the final layer applied was anionic. Haidar *et al.* (7) undertook similar investigations with nanoparticles, preparing core-shell nanoparticles via the layer-by-layer (L-b-L) self-assembly technique for the delivery of biomacromolecules. Their characterization of the size and surface charge following sequential layering revealed that the size of their basic unilamellar liposome was 180 ± 10.5 nm *versus* 345 ± 10.9 nm for liposomes coated with six alternating polyelectrolyte layers of alginate and chitosan. They also noted a decrease in particle size in the two initial layers due to diffusion of the shorter alginate chains between the longer chitosan chains as a result of strong ionic electrostatic interaction and complexation of the polymers to form a dense network. Zeta potentials obtained in the study of Haidar *et al.* (7) inverted significantly between a positive and negative surface charge with the adsorption of each layer, being in the order of 36.6 ± 2.9 mV.

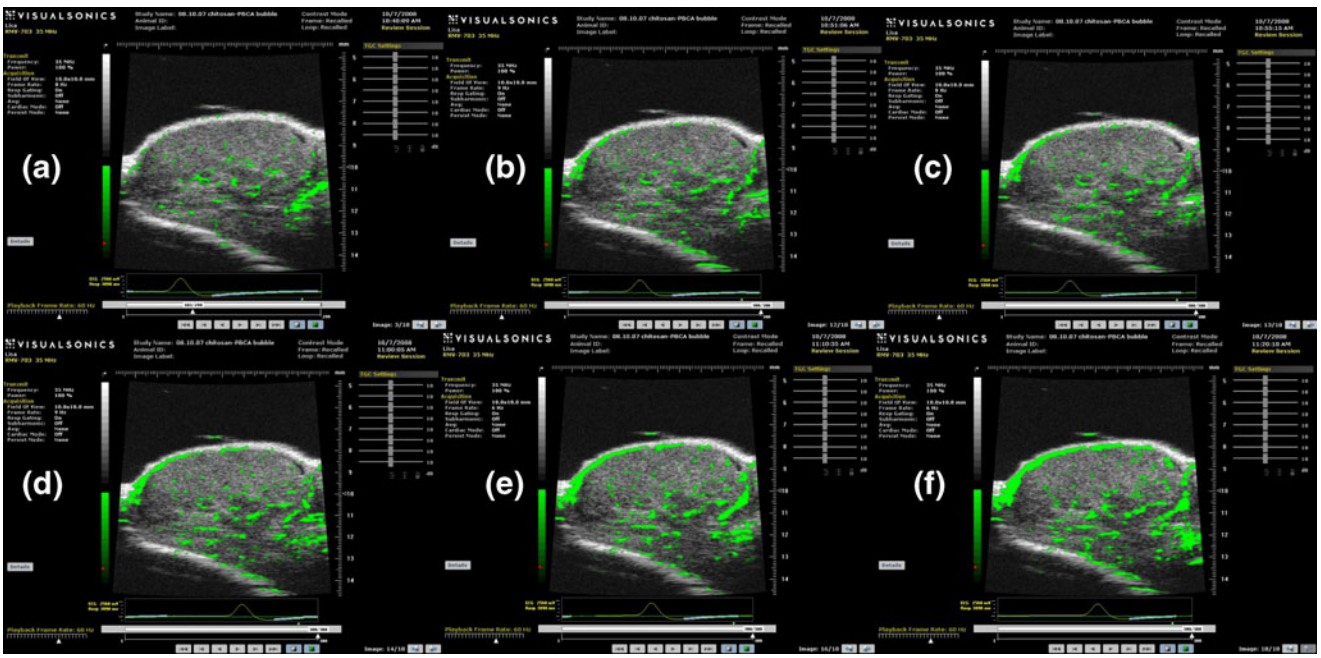

Figure 4 Vascular contrast enhancement following injection of formulation B2 into the subiliac lymph node of the MRL/lpr mouse at (**a**) 1 min, (**b**) 5 min, (**c**) 10 min, (**d**) 20 min, (**e**) 30 min, (**f**) 40 min.

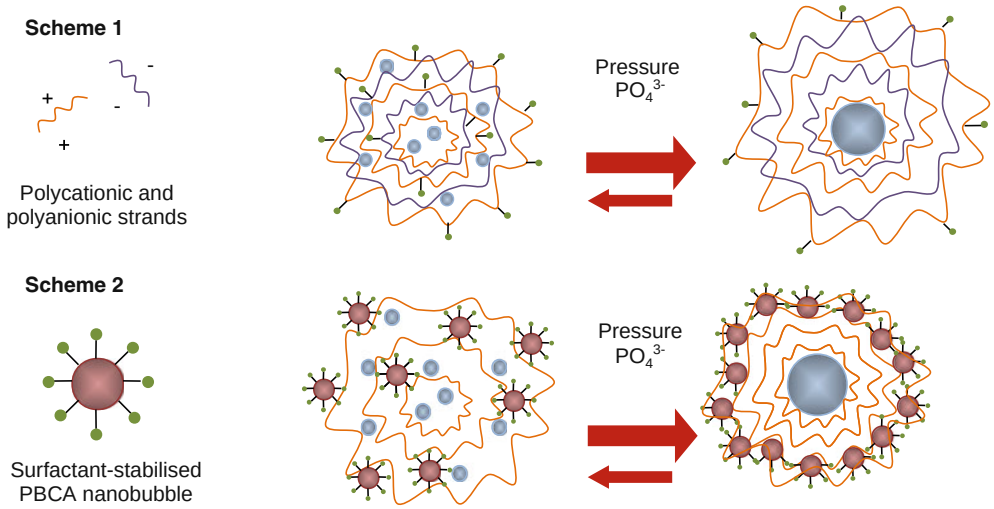

Figure 5 Transitory configurations (re-configuration) of polyionic hydrogel bubbles. Scheme 1 represents the formation of micro-/nanobubbles following the sonication of biopolymer solutions (i.e. chitosan and alginate). Scheme 2 represents the formation of micro-/nanobubbles following sonication of PBCA nanobubbles and the polycationic solution. The configuration is proposed to shift to the right *in vivo* with the resultant observation of enhanced echogenicity and contrast.

Polyionic Hydrogel Bubble Characterization

All the polymeric formulations demonstrated good system stability attested by their fairly negative surface charge and would be suitably applied for organ imaging and certain drug delivery applications (25)

The chitosan-PBCA system (formulation B2) clearly demonstrated a suitable size distribution (~200 nm after 60 min) and could serve as a candidate system for tissue imaging and targeting via the EPR effect (26).

Bubble Lifetime with Reference to Basic Lipobubbles

Polymer-Coated Lipobubble Characterization

The changes in lipobubble lifetime were not significant ($P=0.0634$). Proposedly, the adsorption of polysaccharides such as chitosan over liposomal membranes is due to an initial diffusion-controlled process by the polymeric components, followed by lateral diffusion and subsequent interdigitation (interlocking) of adsorbed polysaccharide molecules into bilayers (27). However, the reason for the thermodynamic instability of this polysaccharide anchoring by adsorption for subsequent liposomal coating may lie in Sihorkar and Vyas's (27) explanation. Their rationalization is threefold: i) the polysaccharides adsorbed on the liposomal surfaces easily desorb/delodge on dilution or on mechanical agitation, ii) peptization or coagulation of the polysaccharides could lead to subsequent destabilization of the liposomal bilayer, and iii) stoichiometric ligand density is often non-reproducible.

There was a negative correlation between bubble size and lifetime ($R^2=-0.72$). This indicates that a more compact structure possessing a smaller diameter and formed by tight interdigitation of the polymer with the phospholipid bilayer and interpenetration of consecutive polymeric layers demonstrated enhanced persistence within the lymph node vasculature.

Noteworthy is that formulations possessing a higher ratio of anionic:cationic coats (A3, A4, A5) and, therefore, a highly anionic overall surface charge (−20.62 mV to −17.54 mV) possessed an enhanced lifetime. This is confirmed by the negative correlation ($R^2=-0.63$) between the zeta potentials and bubble lifetimes measured (Table 3). The final surface charge will ultimately impact on the microvascular retention of the bubbles. The study of Fisher *et al.* (28) was the first to show that a net negative shell charge can result in capillary retention of bubbles within the normal microcirculation via a mechanism other than lodging. Enhanced retention will ultimately result in a comparatively increased resonance and thus more prolonged vascular opacity for these formulations.

To our knowledge, other studies have not significantly reported on the transformation of layered liposomal assemblies into nanobubbles. Investigations reporting on the lifetimes of such systems are limited, thus motivating the need for further studies at enhancing this approach for application to long-circulating nanobubbles.

Polyionic Hydrogel Bubble Characterization

With reference to the polyionic hydrogel bubbles, there was some dampening of the resonance, notably within the first few minutes of injection. This could be due to the presence of a diffuse polymeric hydrogel shell (Figures 3a and 4a). Essentially, the formed species are proposed to have a porous nature (as observed with non-gas-filled nanoparticulate formulations) (29). Upon injection, there is contraction of the polyionic wall due to the presence of hydrodynamic pressure exerted on the bubble wall within the vasculature and complexing ions *in vivo* (Figure 5). This could facilitate a morphological transformation from a porous to a hollow nature upon coalescence of the matrix pores, resulting in the observed enhancement of echogenicity with time as the impedance mismatch between the

blood and the polymeric micro-/nanobubble increases. Thereafter (>5 min), the contrast attained within the lymph node was increasingly favorable. A clear image of the vasculature and extended bubble lifetimes was acquired for the polyionic hydrogel bubbles, demonstrating the enhanced persistence and resilience of these systems as compared to the unmodified basic lipobubble. This may be attributed to the highly flexible, interconnected hydrogel shell which minimizes gas leakage. The prolonged contrast signal may also be attributed to a degree of polymeric deposition/endothelial attachment. The polyionic hydrogel bubble system combines the advantages of a hydrogel system, which include hydrophilicity and flexibility, making cracking of the bubble shell with rapid escape of incorporated gas less likely. Instead, gas diffusion will depend on the swelling of the interconnected bubble shell formed by ionic interaction of the oppositely charged hydrogels. The flexible shell provides enhanced echogenicity with prolonged opacification of the lymph node vasculature. The observed signal is in opposition to that observed for the unmodified lipobubble, which displays enhanced contrast initially, but the signal dissipates after less than 10 min due to nanobubble destruction. For these hydrogel systems, there was a strong negative correlation between bubble size and lifetime ($R^2 = -0.99$), indicating that a smaller, more compact structure demonstrated enhanced persistence and resonance within the lymph node vasculature. There was a good positive correlation between the zeta potential and lifetime of the bubbles ($R^2 = 0.88$). There was a general increase in bubble lifetime as the zeta potential became less negative; however, this could be attributed, to a greater extent, to the polymers implicated in bubble fabrication than to the overall surface charge, as this was favorably anionic for all hydrogel formulations. The improvement in bubble lifetime was significant when a purely polyionic hydrogel bubble shell was instituted compared to the unmodified basic lipobubble (control) ($P = 0.004$).

CONCLUSION

The aim of this study was to investigate various polymeric approaches for their effect on nanobubble size, stability (in terms of surface charge) and potential to enhance bubble life time.

In the first approach, basic and polymerically enhanced lipobubbles were coated with various combinations of polymers. Although the lipobubble lifetime was somewhat enhanced by the physical LbL approach, the improvement was not significant compared to the unmodified lipobubble. There may have been disruption of the polymeric coat during lipobubble creation or on exposure to hydrodynamic pressure *in vivo*. Furthermore, the rigidity of the liposomal coat itself may have been insufficient to support the polymeric layering on gas encapsulation.

The second approach that employed biodegradable, biocompatible polymers with multifunctional capabilities via a simplified, safe and inexpensive technique produced an echogenic, persistent bubble species, Compared to previously investigated polymeric bubbles with their inherent disadvantages, the polyionic hydrogel bubble system combines the advantages of a hydrogel system, which include hydrophilicity and flexibility, making rapid escape of incorporated gas less likely. Instead, gas diffusion will depend on the swelling of the interconnected bubble shell formed by ionic interaction of the oppositely charged hydrogels. The flexible shell provides enhanced echogenicity with prolonged opacification of the lymph node vasculature. Bubble lifetime was significantly enhanced compared to unmodified lipobubbles.

This study has therefore identified the relevance of polymeric modifications to nanobubbles for an improved circulating lifetime, which would be essential for application of these systems in passive drug or gene targeting via the enhanced permeability and retention effect. Further studies on the polyionic hydrogel nanobubble are ongoing for formulation optimization.

ACKNOWLEDGMENTS

This research was funded by the Asia-Africa Program, Tohoku University, Goho Life Sciences International Fund, and National Research Foundation of South Africa.

REFERENCES

1. Hernot S, Klibanov AL. Microbubbles in ultrasound-triggered drug and gene delivery. Adv Drug Deliv Rev (Ultrasound in Drug and Gene Delivery). 2008;60:1153–66.
2. Kodama T, Tomita N, Horie S, Sax N, Iwasaki H, Suzuki R, *et al.* Morphological study of acoustic liposomes using transmission electron microscopy. J Electron Microsc. 2010;59:187–96.
3. Takeuchi H, Yamamoto H, Toyoda T, Toyobuku H, Hino T, Kawashima Y. Physical stability of size controlled small unilameller liposomes coated with a modified polyvinyl alcohol. Int J Pharm. 1998;164:103–11.
4. Walker HW, Grant SB. Influence of surface charge and particle size on the stabilization of colloidal particles by model polyelectrolytes. Colloids Surf A-Physicochem Eng Asp. 1998;135:123–33.
5. Bogdanovic G, Sennerfors T, Zhmud B, Tiberg F. Formation and structure of polyelectrolyte and nanoparticle multilayers: effect of particle characteristics. J Colloid Interface Sci. 2002;255:44–51.
6. Yap HP, Quinn JF, Ng SM, Cho J, Caruso F. Colloid surface engineering via deposition of multilayered thin films from polyelectrolyte blend solutions. Langmuir. 2005;21:4328–33.
7. Haidar ZS, Hamdy RC, Tabrizian M. Protein release kinetics for core-shell hybrid nanoparticles based on the layer-by-layer

assembly of alginate and chitosan on liposomes. Biomaterials. 2008;29(9):1207–15.
8. Decher G. Fuzzy nanoassemblies: toward layered polymeric multicomposites. Science. 1997;277:1232–7.
9. Feinstein SB, Lang RM, Dick C, Neumann A, Al-Sadir J, Chua KG, *et al.* Contrast echocardiography during coronary arteriography in humans: perfusion and anatomic studies. J Am Coll Cardiol. 1988;11:59–65.
10. Shapiro JR, Reisner SA, Lichtenberg GS, Meltzer RS. Intravenous contrast echocardiography with use of sonicated albumin in humans: systolic disappearance of left ventricular contrast after transpulmonary transmission. J Am Coll Cardiol. 1990;16:1603–7.
11. Wheatley MA, Schropet B, Shen P. Contrast agents for diagnostic ultrasound: development and evaluation of polymer-coated microbubbles. Biomatenals. 1990;11:713–8.
12. Kwok KK, Groves MJ, Burgess DJ. Production of 5–15βm diameter alginate-polylysine microcapsules by an air-atomization technique. Pharm Res. 1991;8:341–4.
13. Schneider M, Bussat P, Barrau M-B, Arditi M, Yan F, Hybl E. Polymeric microballoons as ultrasound contrast agents: Physical and ultrasonic properties compared with sonicated albumin. Invest Radiol. 1992;27:134–9.
14. Cohen S, Andrianov AK, Wheatley M, Allcock HR, Langer RS. Gas-filled polymeric microbubbles for ultrasound imaging. United States Patent 5487390, 1996.
15. Matsumura Y, Maeda H. A new concept for macromolecular therapeutics in cancer-chemotherapy—mechanism of tumoritropic accumulation of proteins and the antitumor agent smancs. Cancer Res. 1986;46:6387–92.
16. Agnihotri SA, Mallikarjuna NN, Aminabhavi TM. Recent advances on chitosan-based micro- and nanoparticles in drug delivery. J Control Release. 2004;100:5–28.
17. Douglas KL, Tabrizian MJ. Effect of experimental parameters on the formation of alginate–chitosan nanoparticles and evaluation of their potential application as DNA carrier. J Biomater Sci, Polym Ed. 2005;16:43–56.
18. Motwani SK, Chopra S, Talegaonkar S, Kohli K, Ahmad FJ, Khar RK. Chitosan–sodium alginate nanoparticles as submicroscopic reservoirs for ocular delivery: formulation, optimisation and *in vitro* characterisation. Eur J Pharm Biopharm. 2008;68:513–25.
19. Heskins M, Guillet JE. Solution properties of poly(*N*-isopropylacrylamide). J Macromol Sci Chem. 1968;A2:1441–55.
20. Chung JE, Yokoyama M, Yamato M, Aoyagi T, Sakurai Y, Okano T. Thermo-responsive drug delivery from polymeric micelles constructed using block copolymers of poly(*N*-isopropylacrylamide) and poly(butylmethacrylate). J Control Release. 1999;62:115–27.
21. Murphy ED, Roths JB. Autoimmunity and lymphoproliferation: induction by mutant gene lpr, and acceleration by a male-associated factor in strain BXSB mice. New York: Elsevier North Holland Inc.; 1978.
22. O' Doherty M. Liposome literature review. Nanobiotechnology and Bioanalysis Group, 2004.
23. Schmidt W, Roessling G. Novel manufacturing process of hollow polymer microspheres. Chem Eng Sci. 2006;61:4973–81.
24. Palmowski M, Huppert J, Ladewig G, Hauff P, Reinhardt M, Mueller M, *et al.* Molecular profiling of angiogenesis with targeted ultrasound imaging: early assessment of antiangiogenic therapy effects. Mol Cancer Ther. 2008;7:101–9.
25. Saxena V, Sadoqi M, Kumar S, Shao J. Tiny Bubbles—Multifunctional nanoparticles promise early noninvasive tumor detection and tumor destruction within the body. Nanotechnology. Oemagazine, September 2004. http://spie.org/x16543.xml?ArticleID=x16543.
26. Maeda H, Wu J, Sawa T, Matsumura Y, Hori K. Tumor vascular permeability and the EPR effect in macromolecular therapeutics: a review. J Control Release. 2000;65:271–84.
27. Sihorkar V, Vyas SP. Biofilm consortia on biomedical and biological surfaces: delivery and targeting strategies. Pharm Res. 2001;18:1247–54.
28. Fisher NG, Christiansen J, Leong-Poi H, Jayaweera AR, Lindner JR, Kaul S. Myocardial and microcirculatory kinetics of BR-14, a novel third generation intravenous contrast agent. J Am Coll Cardiol. 2002;39:930–7.
29. Jin M, Zheng Y, Hu Q. Preparation and characterization of bovine serum albumin alginate/chitosan microspheres for oral administration. Asian J Pharm Sci. 2009;4:215–20.